Environ. Sci. Technol. **2004**, *38,* 2142−2152

Fugacity-Based Indoor Residential Pesticide Fate Model

DEBORAH H. BENNETT*,† AND EDWIN J. FURTAW, JR.‡

School of Public Health, Harvard University, Landmark Center, P.O. Box 15677, Boston, Massachusetts 02215, and U.S. Environmental Protection Agency, Las Vegas, Nevada

Dermal and nondietary pathways are possibly important for exposure to pesticides used in residences. Limited data have been collected on pesticide concentrations in residential air and surfaces following application. Models may be useful for interpreting these data and to make predictions about concentrations in the home for other pesticides based on chemical properties. We present a dynamic mass-balance compartment model based on fugacity principles. The model includes air (both gas phase and aerosols), carpet, smooth flooring, and walls as model compartments. Six size fractions of particulate matter with different fate and transport properties are included. We determine the compartmental fugacity capacity and mass-transfer rate coefficients between compartments. We compare model results to chlorpyrifos air and carpet measurements from an independent study. For a comparison, we run the same simulation for diazinon and permethrin. We quantify the effect of parameter uncertainty and model uncertainties related to the source release rate and conduct a sensitivity analysis to determine which parameters contribute most to output uncertainty. In the model comparison to chlorpyrifos measurements, the model results are of the same order of magnitude as measured values but tend to overpredict the measured data, thus indicating the need for a better understanding of emissions from treated surfaces.

Introduction

Screening-level assessments have indicated that dermal and nondietary pathways are potentially important for exposure to pesticides used in homes, especially during the first few days following an application (*1*, *2*). Of particular note are dermal contact with treated surfaces by hands as well as other exposed skin; ingestion from both hand-to-mouth activities and contact with toys and other items that accumulate pesticide; and sorption of pesticides onto food, both from air-to-food transfers and from contact of the food with pesticide residue on surfaces (*3*, *4*).

Among the many parameters needed to characterize exposure to pesticide residues in homes, the time histories of air concentrations and surface concentrations, or loadings, are vital. Some data have been gathered on pesticide concentrations in homes following application but only for a limited number of pesticides (*5*−*9*). There is constant change in the pesticides being used in residences as new pesticides are developed and as regulations change. This creates a demand for models that can be used to predict the time history and fate of a broad range of pesticides based on their chemical properties.

To date, attempts to develop models to predict chemical behavior in indoor environments of pesticides and volatile compounds have been limited by insufficient data to calibrate the model parameters (*10*−*12*). For example, researchers in Japan completed a fugacity-based house model for several types of pesticide applications (*11*). They used a one-room house and included air, walls, and floors as compartments. They considered three sizes of pure phase droplets. However, many of the partition coefficients and transport rates in their model are not supported by previous experimental results. They compared their results to experiments using residential spraying into the air of D-tetramethrin and D-resmethrin. Experiments were also completed for treatment of floors and walls using D-phenothrin and D-tetramethrin. Only limited data were collected on surface concentrations, with more collected for air for the comparisons.

In 1993, Neretnieks et al. (*12*) proposed a 21-compartment model of a typical office to examine exposure to compounds leaching out of the flooring. The model included two boundary layers for the resistance, with many surface materials divided into multiple layers. However, they based many parameter values on best judgment. There was no comparison with experimental results.

A greater body of research is available on the sink effect (i.e., the partitioning of compounds between air and indoor material surfaces such as vinyl, wallboard, or carpet) and on rates of sorption to and desorption from such surface materials (*12*−*25*). However, several challenges still exist for modeling partitioning to surfaces. It is not established whether a chemical partitions primarily onto the surface of a material (*13*) or whether the compounds diffuse into the pores and/or body of the material (*16*). Additionally, partitioning and diffusion may occur on different time scales, with short-term experiments accounting for partitioning onto the surface and long-term experiments accounting for diffusion into the material. Presently, insufficient data are available to develop models that account for the diffusion into the materials. Another key issue is whether partitioning onto surfaces is a reversible or irreversible process. While most experiments have assumed reversibility, some compounds have irreversible partitioning onto surfaces (*22*).

Jorgensen et al. (*19*) proposed three general criteria for developing models of surfaces: (i) models should be based on sound physical/chemical description of the process (i.e., theoretically derived models are preferred over empirical models), (ii) models should be mathematically as simple as possible, and (iii) the model should "adequately" fit measured data. As described in the model development section, we found that fugacity-based models are well-suited to meeting these criteria.

Fugacity is linearly related to concentration and can be regarded physically as the partial pressure or escaping potential exerted by a chemical in one physical phase on another (*26*). Fugacity, f (Pa), is linearly related to mass by fugacity capacity, Z (mol/m^3·Pa), $M = fZV$, where M is the mass of the compound in the compartment (mol) and V is the volume of the compartment (m^3). The fugacity capacity defines the holding capacity of a material for a chemical substance based on the properties of both the material and

* Corresponding author phone: (617)384-8812; fax: (617)384-8859; email: dbennett@hsph.harvard.edu.
† Harvard University.
‡ U.S. Environmental Protection Agency.

10.1021/es034287m CCC: $27.50

Published on Web 02/28/2004

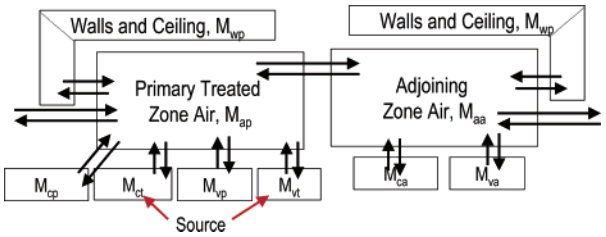

FIGURE 1. Model framework for indoor fugacity model.

the chemical. When two or more compartments are in equilibrium, the fugacity is the same in all phases. Fugacity models can be used to represent a dynamic system with fugacity changing in time due to an imbalance of sources and losses (*26*). The direction of flow is always from regions of higher to lower fugacity.

In this paper, we develop relationships between the chemical properties and the fugacity capacity for indoor surfaces for use in a mass-transport model. The relationship between the chemical properties and the fugacity capacity allows the model to be applied to compounds for which there are no experimental data. Additionally, we reviewed the literature for relevant experimental data that give insight to the transfer rate from air to surfaces, and we use a boundary layer approach to quantify this transfer rate.

In addition to the gas-phase compound, particles must be modeled. Particles can act as a reservoir for storage of a compound, a transport mechanism through deposition and resuspension from surfaces, and an exposure medium for dermal and nondietary ingestion exposure. We have included multiple size fractions of particles in our model, defining them to be relevant for both transport and exposure processes as this model will eventually be linked with an exposure model.

In this paper, we describe the model and present model input values. We present a case study with three compounds, chlorpyrifos (CAS Registry No. 2921-88-2), diazinon (CAS Registry No. 333-41-5), and permethrin (CAS Registry No. 52645-53-1). Chlorpyrifos and diazinon were used extensively in the indoor environment in the past, but they are no longer registered for indoor sources, while permethrin continues to be used in the indoor environment. We compare the chlorpyrifos case to an application in a test home. Monte Carlo simulations are completed to determine the range of uncertainties in the modeled concentrations as well as to complete a sensitivity analysis.

Model Description

The fugacity-based indoor pesticide model is a dynamic mass-balance model with several compartments simultaneously exchanging mass. In this paper, the model is parameterized for the compartments shown in Figure 1. The room or rooms where the pesticide is applied is the pesticide-treated zone, having an air compartment and five surface compartments. Compartments for the carpet and vinyl flooring that are treated with pesticide are included as are three nontreated surface compartments that can act as potential reservoirs for the chemical: carpet, vinyl floor, and walls/ceiling. In this model, we assume a specified thickness for each surface material and further assume that the compound is evenly distributed through the surface material, referred to simply as surfaces in this paper. The remainder of the house is in the adjoining zone, having an air compartment and three surface compartments.

In subsequent sections, we define the mass-balance equations, define the fugacity capacity of each compartment, and define the transfer rates among the compartments. Because we applied a parameter uncertainty analysis to the model results, we assign a mean value and coefficient of variation to each parameter. As a default, we use log-normal distributions to represent parameter variance. If a distribution other than log-normal is used, the form of the distribution is specified.

Mass-Balance Equations. The mass in each compartment is the state variable, and mass transfer between compartments is defined by mass-transfer rate coefficients accounting for both diffusive and advective transfers. The compartment mass is defined by a set of differential equations accounting for all gain and loss processes. The equation for the mass in the air of the primary treated room is

$$\frac{dM_{ap}}{dt} = -L_{ap}M_{ap} + T_{aa\_ap}M_{aa} + T_{ct\_ap}M_{ct} + T_{vt\_ap}M_{vt} + T_{ca}M_{cp} + T_{va}M_{vp} + T_{wa}M_{wp} \quad (1)$$

where M_i is the mass associated with compartment i (g), T values are the transfer factors (1/d), and L_i is the loss-rate constant for compartment i (1/d). The subscript ap is the air compartment in the primary zone (i.e., the zone in which the pesticide is first applied), aa is the air in the adjoining room, ct is treated carpet, vt is treated vinyl, cp is untreated carpet in the primary zone, vp is untreated vinyl in the primary zone, and wp is walls and ceiling in the primary zone. We use T_{aa_ap} for transfers of air from the adjoining to primary zone, T_{ca} for transfer from untreated carpet to air, T_{ct_ap} for transfer from treated carpet to air, T_{va} for untreated vinyl to air, T_{vt_ap} for treated vinyl to air, and T_{wa} for walls to air. The loss-rate constant is the sum of all loss and transfer processes:

$$L_{ap} = k_a + T_{ap\_out} + T_{ap\_aa} + T_{ap\_ct} + T_{ap\_vt} + T_{ap\_cp} + T_{ap\_vp} + T_{ap\_wp} \quad (2)$$

where k_a is the degradation rate constant in air and the other transfer factors are T_{ap_out} for air to outdoors, T_{ap_aa} for air to the adjoining room, T_{ap_ct} for air to treated carpet, T_{ap_vt} for air to treated vinyl, T_{ap_cp} for air to untreated carpet, T_{ap_vp} for air to untreated vinyl, and T_{ap_wp} for air to walls.

Similar to eq 1, a differential equation describes the mass in air in the adjoining room:

$$\frac{dM_{aa}}{dt} = -L_{aa}M_{aa} + T_{ap\_aa}M_{ap} + T_{ca}M_{ca} + T_{va}M_{va} + T_{wa}M_{wa} \quad (3)$$

where the subscript ca is carpet, va is vinyl, and wa is walls and ceiling, all in the adjoining room. The loss-rate constant is defined as:

$$L_{aa} = k_a + T_{aa\_out} + T_{aa\_ap} + T_{aa\_ca} + T_{aa\_va} + T_{aa\_wa} \quad (4)$$

where the transfer factors are defined as T_{aa_out} for air to outdoors, T_{aa_ca} for air to carpet, T_{aa_va} for air to vinyl, and T_{aa_wa} for air to walls.

The mass associated with each of the surfaces is also described by a differential equation. In the subscript jk, the first letter refers to the compartment type (a for air, c for carpet, v for vinyl, and w for wall), and the second letter refers to a specific rendition of that surface (t for treated surfaces, p for untreated surfaces in the primary treated room, and a for surfaces in the adjoining room). We refer to the two letters as j and k and write the general form of the mass balance equation for surfaces as:

$$\text{surfaces: } \frac{dM_{jk}}{dt} = -L_jM_{jk} + S_{jt} + T_{ak\_jk}M_{ak}; \quad L_j = k_j + T_{ja} \quad (5)$$

TABLE 1. Input Parameters, Mean Value, and Coefficient of Variation[a]

property name (units)	symbol	mean value	CV
temperature (K)	T_m	298	0.20
air exchange rate (1/d)	AE	18	1.16
room air exchange rate (1/d)	RA	72	0.30
particle density (kg/m^3)	ρ_d	1500	0.25
thickness of organic film (m)	δ_{film}	1.0×10^{-7}	0.80
organic matter in films	$f_{oc,f}$	0.2	0.50
film density (kg/m^3)	ρ_f	1200	0.20
carpet thickness (m)	δ_c	1.0×10^{-2}	0.50
vinyl thickness (m)	δ_v	5.0×10^{-4}	0.50
wall thickness (m)	δ_w	5.0×10^{-3}	0.50
horizontal deposition rate coeff., 0−1 μm (1/d)	$v_{h,1}$	2.4	0.30
dust loading on carpet (kg/m^2)	ρ_c	1.0×10^{-2}	0.75
dust loading on hard floor (kg/m^2)	ρ_v	8.5×10^{-5}	0.20
boundary layer thickness (m)	δ_{bl}	3.3×10^{-2}	0.77
OH radical concentration (molecules/cm^3)	C_{OH}	1.1×10^5	0.33

[a] References for each parameter are given in the Supporting Information.

where k_j is the transformation rate constant of the chemical on the surface, and S_{jt} (g/d) is the application rate of the chemical to the treated surfaces. As an example, the equation for the treated carpet is

$$\text{treated carpet: } \frac{dM_{ct}}{dt} = -L_c M_{ct} + S_{ct} + T_{ap\_ct} M_{ap}; \quad L_c = k_c + T_{ct\_ap} \quad (6)$$

There is a specific equation in this format for each surface.

Fugacity Capacities. For each compartment, we define the fugacity capacity. In the case that a compartment is comprised of two phases, for example, the gas phase and the particle phase in air, we define the fugacity capacity of each phase and sum them based on the volume fraction of each phase, implicitly assuming that the multiple phases are in equilibrium.

Air Compartment. The air compartment is comprised of both pure air and particles. We consider several size fractions of particles and sum across all size fractions. The fugacity capacity of pure air (Z_{air}, mol/ m^3·Pa) is

$$Z_{air} = \frac{1}{R_c \times T_m} \quad (7)$$

where R_c is the ideal gas constant (8.314 Pa·m^3/mol·K) and T_m is the ambient temperature (K) as listed in Table 1 along with the other environmental input parameters.

Recently, approaches have been developed by Finizio et al. (*30*) and Harner and Bidleman (*31*) relating the air−particle partition coefficient to the octanol−air partition coefficient, K_{oa} (unitless). K_{oa} can be measured or calculated as a ratio of the octanol−water and air−water partition coefficients:

$$K_{oa} = \frac{K_{ow} \times R_c T_m}{H}. \quad (8)$$

where H is the Henry's law constant (Pa·m^3/mol) and K_{ow} is the octanol−water partition coefficient (unitless). The partition coefficient between particles and air, K_p (m^3/μg), is defined as the ratio of mass associated with 1 μg of particulate matter to the mass in 1 m^3 of air (m^3/μg). We specify the size fraction for the particle−air partition coefficient with the subscript i. Approaches for air−particle partitioning are summarized in Bennett et al. (*32*). We select the Harner and Bidleman (*31*) relationship for the partition coefficient:

$$\log K_{p,i} = \log K_{oa} + \log\left(\frac{f_{oc,i}}{0.74}\right) - 11.91 \quad (9)$$

where $f_{oc,i}$ is the fraction of organic carbon for particles in a specific size fraction. Little is known regarding the size distribution of the fraction of organic carbon. One study determined elemental and organic carbon in urban regions for various size fractions (*33*). Two studies have measured the overall organic carbon fraction of house dust, found to be consistently 19% across a number of homes in one study (*34*) and 40% in a second study (*35*). The first study listed is newer and uses improved experimental methods. Therefore, 19% was chosen as the total fraction of organic carbon. Size-specific fraction of organic carbon values was determined based on trends in outdoor levels. These values along with all other properties for the particulate matter are listed in Table 2.

The fugacity capacity for air particles of size fraction i ($Z_{ap,i}$ in mol/m^3·Pa) is

$$Z_{ap,i} = \frac{K_{p,i} \times \rho_d \times 10^9}{R_c \times T_m} \quad (10)$$

where ρ_d is the dust particle density (kg/m^3) and the factor 10^9 is included to convert the units from kilograms to micrograms. The fugacity capacity for the air compartment is volume averaged between the air and each particle phase:

$$Z_a = \sum_{i=1}^{i=6} \frac{Z_{ap,i} \times \rho_{p,i}}{\rho_d \times 10^9} + Z_{air} \quad (11)$$

where $\rho_{p,i}$ is the particle mass concentration in the air for a given size fraction (μg/m^3) and 10^9 is again included as a conversion factor. The concentrations of various size fractions are approximated from measured and modeled data and are listed in Table 2 (*36*, *37*).

Surface Compartments. Published experimental work provides information to establish sorption and desoprtion rates from surfaces (*12*−*25*). Experiments have traditionally been done by releasing a low concentration of the compound of interest into a nonreactive chamber with a sample of the material of interest, followed by a desorption period. The air concentration throughout the experiment is measured, and from this, adsorption, desorption, and partition coefficients can be derived. The following equations describe the mass balance:

$$V\frac{dC_g}{dt} = Q_g C_{g,in} - Q_g C_g - k_s C_g A + k_d M^n A \quad (12)$$

$$\frac{dM}{dt} = k_s C_g - k_d M^n \quad (13)$$

where C_g is the concentration of the chemical in the chamber air (mg/m^3), $C_{g,in}$ is the concentration in the inlet air (mg/m^3), V is the chamber volume (m^3), Q_g is the flow rate through the chamber (m^3/h), A is the area of the sink material (m^2), k_s is the adsorption coefficient (m/h), k_d is the desorption rate coefficient, and M is the mass on the sink material per unit area (mg/m^2). If we assume linear sorption, n is equal to 1, and k_d has units of 1/h. In this case, the flux from air to surfaces is

$$\text{flux} = k_s C_g - k_d M \quad (14)$$

where flux is on a per area basis (mg/m^2·h). The air and surface are in equilibrium when the net flux is equal to zero.

TABLE 2. Properties of Dust in Various Size Fractions and Mean Values with Coefficient of Variation in Parentheses[a]

particle size fraction,[b] j (μm)	fraction of org carbon, $f_{oc,j}$ (unitless)	particulate mass concn in air, $\rho_{p,j}$ (μg/m^3)	vertical deposition rate coeff, $v_{v,j}$ (1/d)	resuspension rate coeff, $v_{r,j}$ (1/d)	fraction in size fraction: hard floor, $f_{v,j}$ (unitless)	fraction in size fraction: carpet, $f_{c,j}$ (unitless)
0−1	0.35(0.3)	9.5 (0.8)	2.4 (0.3)	2.6×10^{-6} (1.0)	0.02 (1.0)	0.01 [0.001,0.013][c]
1−2.5	0.3 (0.3)	2.4 (0.85)	10.8 (0.3)	1.1×10^{-5} (1.0)	0.02 (1.0)	0.01 [0.001,0.013][c]
2.5−10	0.3 (0.3)	7.6 (0.8)	24 (0.3)	1.6×10^{-4} (1.0)	0.09 (0.5)	0.06 [0.03,0.09][c]
10−65	0.2 (0.2)	2.0 (0.5)	2400 (0.3)	6.9×10^{-4} (1.0)	0.71[d]	0.27 [0.24,0.3][c]
65−150	0.15 (0.2)	0.095 (0.5)	24000 (0.3)	1.0×10^{-4} (1.0)	0.06 (2.0)	0.27[d]
150−2000	0.05 (0.25)	0(0)		1.0×10^{-4} (1.0)	0.1 (1.0)	0.38[d]

[a] References for each parameter are given in the Supporting Information. [b] Based on aerodynamic diameter. [c] These distributions are uniform, and the values in the brackets indicate the minimum and maximum values. [d] Instead of distributions, these values are determined based on remaining fraction of the dust.

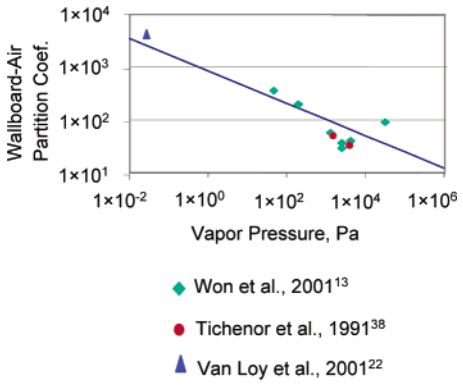

FIGURE 2. Surface partition coefficient for wallboard vs vapor pressure from multiple experiments. Won et al. (*13*) used the following compounds in all experiments: MTBE, cyclohexane, 2-propanol, toluene, tetrachloroethane, ethylbenzene, *o*-dichlorobenzene, and 1,2,4-trichlorobenzene. Tichenor et al. (*38*) used tetrachloroethane and ethylbenzene. Van Loy et al. (*22*) used phenanthrene.

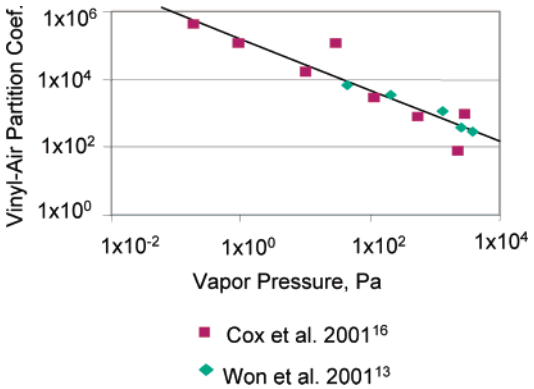

FIGURE 3. Surface partition coefficient for vinyl vs vapor pressure from multiple experiments. Cox et al. (*15*, *16*) used water, 1-butanol, toluene, phenol, *n*-decane, *n*-dodecane, *n*-tetradecane, and *n*-pentadecane in their experiments.

In this case, an equilibrium partition coefficient is defined as:

$$K_{eq} = \frac{k_s}{k_d} = \frac{M}{C_g} \quad (15)$$

where K_{eq} has units (m). Since we are using surface compartments, we define a thickness for the material and define a surface−air partition coefficient, K_{ja} (unitless), which is K_{eq} divided by the thickness of the surface, d_j (m). The fugacity capacity of the surface j can then be calculated as:

$$Z_j = \frac{k_s/k_d}{R_c \times T_m \times d_j} = \frac{K_{ja}}{R_c \times T_m}. \quad (16)$$

We now discuss each surface and relationship between K_{ia} and the chemical properties.

Wallboard. To establish a relationship between the painted wallboard-to-air partition coefficient and chemical properties, we consolidate data from several sources (*13*, *22*, *38*) [nicotine data from Van Loy et al. (*22*) were not included due to potential surface reactions]. By including several sets of measured partitioning relationships, we obtained more compounds for correlating partitioning with chemical properties and can compare studies for consistency. For surface−air partition coefficients, we used both vapor pressure (VP) and K_{oa} as predictors of surface partitioning and found a better correlation for VP. Figure 2 is a plot of the wallboard−air partition coefficient versus the vapor pressure for the available chemicals. As shown in the following equation, a regression line was fit to the observed relationship between K_{wa} and log VP:

$$K_{wa} = \frac{k_s/k_d}{d_w} = 10^{2.93-0.31 \log VP}; \quad R^2 = 0.85 \quad (17)$$

which is used to calculate the fugacity capacity using eq 16.

Vinyl Flooring. Several studies have evaluated vinyl−air partition coefficients. Cox et al. (*16*) determined the partition coefficient and the diffusion coefficient into vinyl flooring by continually weighing a sample with a microscale to determine what mass of compound had partitioned into the material when in a chamber at a fixed air concentration. Won (*39*) used the air and surface chamber system described above to determine partitioning rates into vinyl. The units on the partition coefficients calculated by the two methods differed, but we were able to convert them to the same units, as described in the Supporting Information. The mass-based partition coefficients are plotted in Figure 3 versus the vapor pressure. The resulting correlation equation is

$$K_{va} = \frac{k_s/k_d}{d_v} = 10^{5.2-0.68 \log VP}; \quad R^2 = 0.80. \quad (18)$$

Diamond et al. (*40*) indicate that an organic film builds up on impermeable surfaces. The film develops based on particle deposition and deposition of various gases. Once the film has developed, there is gas-phase partitioning to the film. We need to include the fugacity capacity of this phase in the overall hard-flooring compartment. The fugacity capacity of the organic film (Z_{film}, mol/m^3·Pa) is based on the organic carbon partition coefficient (*40*) using the following

equation, explained in the Supporting Information:

$$Z_{film} = \frac{0.48 \times K_{ow} \times f_{oc,f} \times \rho_f}{H \times 1000} \quad (19)$$

where $f_{oc,f}$ is the fraction of organic material in the film (unitless), ρ_f is the density of the film (kg/m^3), and 1000 is a conversion factor with units of L/m^3. Distributions used for the properties of the film are listed in Table 1. There is also dust on vinyl surfaces that must be included in the fugacity capacity for vinyl surface and is discussed later in the paper.

Carpet. Carpet has been found to be a potential reservoir for pesticides in the home. The typical carpet consists of carpet fibers, either wool or nylon, a carpet backing, generally consisting of polypropylene, and a carpet cushion, typically polyurethane. Although the carpet system is comprised of different components, we treat them as one compartment because there are insufficient data to consider them separately.

Several recent experiments provide insight on the magnitude of K_{ca}. Won et al. (*14*) ran a series of chamber experiments for carpet as well as a carpet and pad system. They reported higher partition coefficients in the system that includes both carpet and pad. Both Van Loy et al. (*22*) and Tichenor et al. (*38*) took a similar experimental approach. Meininghaus et al. (*21*) completed a series of experiments looking at both the diffusion through a material and the partitioning into that material. They had a two-chamber system and measured the concentrations on both sides of the material.

We considered the data from all of these experiments, as discussed in the Supporting Information, and selected a partition coefficient as a function of VP based on the data measured by Won et al. (*14*) for carpet with no pad:

$$K_{ca} = \frac{k_s/k_d}{d_w} = 10^{3.82-0.62 \log VP} \quad (20)$$

Particulate matter must also be included in this compartment, as discussed below.

Particulate Matter. The fugacity capacity of the overall carpet and vinyl compartments includes the fugacity capacity of the dust on these surfaces. This depends on both the total mass of dust on each surface as well as the percent in each size fraction, as the organic content and thus fugacity capacity vary by size. The details on the development of each of these parameters can be found in the Supporting Information, with a summary presented in this section.

Dust composition and behavior vary by size fraction, and thus multiple size fractions are considered in the model. Indoor dust composition differs from outdoor dust composition as indoor dust is made up of particles from cooking, flakes from skin and other indoor sources, and particles of outdoor origin, while outdoor dust is primarily composed of crustal material and combustion byproducts. The fraction of organic carbon increases with decreasing size, affecting fugacity capacity and concentration. One study found that concentrations in dust of polycyclic aromatic hydrocarbons (PAHs) and pesticides were highest for the smallest size fractions (*27*). The authors suggest that this results from the higher surface-to-mass ratio for the smaller particles. Another potential explanation is the general trend of increasing fraction of organic carbon with decreasing particle size (*33*).

The ability of a particle to adhere to skin varies by size. It has been estimated that 150 μm is the maximum particle size for transfer of wet soil particles to a dry hand and that 65 μm is an upper limit for dry soils (*28*). Rodes et al. suggest that the maximum size likely to stick to skin is around 100 μm (*29*). On the basis of these factors, we consider dust from 0 to 1, from 1 to 2.5, from 2.5 to 10, from 10 to 65, from 65 to 150, and from 150 to 2000 μm.

Two studies measured the mass of dust on both hard floor and carpets (*41*, *42*). From these studies, we develop a distribution for the mass of dust on vinyl flooring, ρ_v (kg/m^2). Fortune et al. investigated the mass of dust obtained from vacuuming and vacuuming with a beater-bar machine to remove deeply embedded dust in eight homes (*43*). The results indicated that the actual dust loading in carpet was approximately 10 times the amount removed by conventional vacuuming. This was taken into account in developing the distribution of the mass of dust on carpets, ρ_c (kg/m^2).

For hard floors, we determined the volume fraction in each size bin ($f_{v,j}$, unitless) using a 2-week study that assessed the seasonal deposition rates of household dust onto surfaces (*44*). The different houses and seasons were used to develop a distribution for five of the size bins, with the sixth being the remainder, as indicated in Table 2.

Lewis et al. (*27*) determined the fraction of dust in each size fraction for carpets using dust collected from conventional vacuum cleaner bags. Conventional vacuum cleaners are known to be inefficient at collecting dust in the under-2-μm size fraction (*27*), and we assume this size fraction is under-represented in the vacuum bag sample. We develop distributions for the volume fraction ($f_{c,j}$, unitless) in four of the size bins, with the remaining two a function of the remainder.

The total fugacity capacity for the dust is the sum of the fraction of dust in each size bin multiplied by the fugacity capacity for that size dust as calculated in eq 10:

$$Z_{dust,c} = \sum_{i=1}^{i=6} Z_{ap,i} \times f_{c,i}; \quad Z_{dust,v} = \sum_{i=1}^{i=6} Z_{ap,i} \times f_{v,i} \quad (21)$$

The total fugacity capacity of the carpet and hard surfaces are volume weighted between the phases:

$$Z_v = \frac{Z_{film}\delta_{film} + Z_{vinyl}\delta_v + Z_{dust,v}\frac{\rho_v}{\rho_d}}{\delta_{film} + \delta_v + \frac{\rho_v}{\rho_d}};$$

$$Z_c = \frac{Z_{carpet}\delta_c + Z_{dust,c}\frac{\rho_c}{\rho_d}}{\delta_c + \frac{\rho_c}{\rho_d}} \quad (22)$$

Transport Processes. In the subsequent sections, we discuss the transfer factors between compartments. The equations are summarized in Table 3, with additional parameters defined in Table 4.

Movement of Air. Movement of air and indoor aerosols occurs through ventilation with outdoors and exchange between rooms. Both temporal and inter-home variability are considered in estimating the range of ventilation rates. If the contaminant is also found outdoors, the ventilation from outdoors should be considered. For total house ventilation rates, we use the distribution of data analyzed by Murray and Burmaster (*45*) taken from measurements completed by Brookhaven National Laboratory, as listed in Table 1.

Miller et al. (*46*) completed a study of the air-exchange rate between two rooms with an open door under two ventilation conditions, with and without ventilation fans. For the case with no fans, the air-exchange rate between rooms was nearly 2 air exchanges per hour. With the

TABLE 3. Transfer Factors

		advective (1/d)	diffusive (1/d)
air in primary treated room to air in adjacent room	T_{ap_aa}	RA	
air in primary treated room to outdoors	T_{ap_out}	AE	
air in primary treated room to treated carpet	T_{ap_ct}	$\frac{v_v}{h}\left(\frac{Z_{ap}\times\rho_p}{\rho_{ap}\times Z_a}\right)\left(\frac{SA_c}{A_p}\right)$	
air in primary treated room to treated vinyl	T_{ap_vt}	$\frac{v_v}{h}\left(\frac{Z_{ap}\times\rho_p}{\rho_{ap}\times Z_a}\right)\left(\frac{SA_v}{A_p}\right)$	
air in primary treated room to untreated carpet	T_{ap_cp}	$\frac{v_v}{h}\left(\frac{Z_{ap}\times\rho_p}{\rho_{ap}\times Z_a}\right)\left(\frac{ff_cA_p-SA_c}{A_p}\right)$	$\frac{Y_{ac}}{Z_ah}\left(\frac{ff_{ca}A_p-SA_c}{A_p}\right)$
air in primary treated room to untreated vinyl	T_{ap_vp}	$\frac{v_v}{h}\left(\frac{Z_{ap}\times\rho_p}{\rho_{ap}\times Z_a}\right)\left(\frac{ff_vA_p-SA_v}{A_p}\right)$	$\frac{Y_{av}}{Z_ah}\left(\frac{ff_{va}A_p-SA_v}{A_p}\right)$
air in primary treated room to walls	T_{ap_wp}	$\frac{v_h}{^1/_4\sqrt{A_p}}\left(\frac{Z_{ap}\times\rho_p}{\rho_{ap}\times Z_a}\right)$	$\frac{Y_{aw}}{Z_a\,{}^1/_4\sqrt{A_p}}$
air in adjoining room to air in primary treated room	T_{aa_ap}	RA	
air in adjoining room to outdoors	T_{aa_out}	AE	
air in adjoining room to carpet	T_{aa_ca}	$\frac{v_v}{h}\left(\frac{Z_{ap}\times\rho_p}{\rho_{ap}\times Z_a}\right)(ff_c)$	$\frac{Y_{ac}ff_{ca}}{Z_ah}$
air in adjoining room to vinyl	T_{aa_va}	$\frac{v_v}{h}\left(\frac{Z_{ap}\times\rho_p}{\rho_{ap}\times Z_a}\right)(ff_v)$	$\frac{Y_{av}ff_{va}}{Z_ah}$
air in adjoining room to walls	T_{aa_wa}	$\frac{v_h}{^1/_4\sqrt{A_a}}\left(\frac{Z_{ap}\times\rho_p}{\rho_{ap}\times Z_a}\right)$	$\frac{Y_{aw}}{Z_a\,{}^1/_4\sqrt{A_a}}$
carpet to air	T_{ca}	$v_{rc}\frac{Z_{cp}\rho_c}{\rho_{ap}\delta_cZ_c}$	$\frac{Y_{ac}}{Z_c\delta_c}$
vinyl to air	T_{va}	$v_{rv}\frac{Z_{vp}\rho_v}{\rho_{ap}\delta_vZ_v}$	$\frac{Y_{av}}{Z_v\delta_v}$
walls to air	T_{wa}		$\frac{Y_{aw}}{Z_w\delta_w}$

TABLE 4. Test House Parameters[a]

property name (units)	symbol	EPA test house
area of treated zone (m^2)	A_p	30
area of untreated zone (m^2)	A_a	92
height of ceiling (m)	h	2.4
fraction of floor that is carpet, treated room	ff_c	0.67
fraction of floor that is vinyl, treated room	ff_v	0.33
fraction of floor that is carpet, untreated room	ff_{ca}	0.9
fraction of floor that is vinyl, untreated room	ff_{va}	0.1
area of treated surface, vinyl (m^2)	SA_v	0.75
area of treated surface, carpet (m^2)	SA_c	0

[a] Values based on ref *8*.

ventilation fans on, the rate increased to over 5 exchanges per hour. Well-mixed conditions might be applicable when doors are open. We consider two zones and consider the mixing between them, with values listed in Table 1.

Movement of Dust. Limited data are available for indoor resuspension rates. Thatcher and Layton measured resuspension rates between 1.8×10^{-5} and 3.8×10^{-4} per hour for normal activities of four people in a home (*41*). Resuspension rates by particle size fraction were made assuming that all of the mass of dust was available for resuspension. Rhodes et al. (*47*) showed that particles smaller than $\sim 1\,\mu$m were not readily dislodged from carpet fibers during walking events cited in ref *29*, which is consistent with the lower values found in this size fraction by Thatcher and Layton (*41*). We used the data in Thatcher and Layton (*41*) along with our assumptions for mass loading of dust on surfaces and the assumption that the homes are occupied on average 8 h a day to calculate appropriate resuspension rate distributions in Table 2.

Due to the increased dust loading on carpets relative to hard floor, resuspension in this model is approximately 10 times greater from carpeted floors than hard floors. This is greater than differences measured in studies by Ferro et al. (*48*) and Long et al. (*37*), who have shown that doing the same activity on a carpeted surface results in twice the indoor dust level than on a hard surface.

The vertical deposition rate coefficient to horizontal surfaces for size fractions below 10 μm are based on Riley et al. (*36*). For larger size fractions, data are taken from Nazaroff and Alvarez-Cohen (*49*). We do not include filtration through the heating/air conditioning filter. For particles less than 1.0 μm in diameter, the horizontal deposition rate coefficient to vertical surfaces is included (*50*).

Diffusive Transfer Rates to Surfaces. Mass transfer is driven by the fugacity difference between the air and the surface, the movement of air in the room, the resistance to transfer through the air, and the resistance to transfer through the surface. Most of the experiments that have determined the

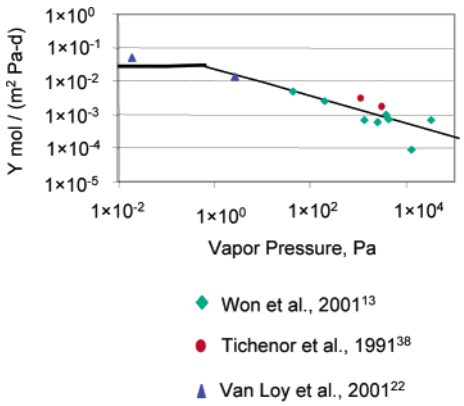

FIGURE 4. Transfer rate vs vapor pressure for partitioning to wallboard.

transfer rates between air and surfaces have used sorption and desorption rates. We determine the flux in terms of the mass in each compartment:

$$\text{flux} = k_s\left(C_{air} - \frac{M}{K_{eq}}\right) = k_s\left(\frac{M_a}{V_a} - \frac{M_j}{AZ_j\delta_j R_c T_m}\right) = \frac{k_s}{R_c T_m}\left(\frac{M_a A}{hZ_{air}} - \frac{M_j}{\delta_j Z_j}\right) \quad (23)$$

where A is the interfacial area between the two compartments (m^2), h is the height of the room (m), and δ_j is the thickness of surface material j (m). We then define a fugacity-based transfer factor between the air and the surface i as Y_{ai} (mol/(m^2Pa·d)), such that the flux and transfer rates to and from the surface are

$$\text{flux} = (T_{aj}M_a - T_{ja}M_j); \quad T_{aj} = \frac{Y_{aj}}{Z_{air}h}; \quad T_{ja} = \frac{Y_{aj}}{Z_j\delta_j} \quad (24)$$

where $Y_{aj} = k_s/R_cT_m$.

In Figure 4, we plot the mass-transfer rate to the wallboard versus vapor pressure from the available experimental data. The data indicate that there is a maximum transfer rate, physically due to the resistance through the air boundary layer. Chemicals with higher vapor pressures exhibit an additional resistance to transfer from the wallboard side of the interface. A line was fit to the data to determine the mass-transfer rate coefficient for the higher volatility compounds:

$$Y_{aw} = 10^{-1.63-0.41\log VP}; \quad R^2 = 0.67 \quad (25)$$

The transfer rate is limited by the mass transfer through the air. The flux can be written as a stagnant boundary layer where the resistance to transfer is determined by the molecular diffusion rate and the boundary-layer thickness:

$$\text{flux} = \frac{D_{air}}{\delta_{bl}}(C_{air,a} - C_{air,s}) \quad (26)$$

where flux has units of mg/m^2·d, D_{air} is the diffusion coefficient in pure air (m^2/d), δ_{bl} is the boundary layer thickness (m), $C_{air,a}$ is the gas-phase concentration in the well-mixed region (mg/m^3), and $C_{air,s}$ is the gas-phase concentration at the surface (mg/m^3). The literature over the years has presented several approaches for determining the appropriate boundary-layer thickness, and these have been summarized in the Supporting Information. We determined the effective boundary layer based on work by Lai and Nazaroff (*50*) as well as Morrison (*51*). We use these values to develop the distribution listed in Table 1.

The equation for the mass-transfer rate (g/d) in terms of the boundary-layer thickness is

$$\text{mass-transfer rate} = A\frac{D_{air}}{\delta_{bl}}\left(\frac{C_{air,s}Z_a}{Z_i} - C_{air,a}\right) = \frac{D_{air}Z_{air}}{\delta_{bl}}\left(\frac{M_j}{Z_j\delta_j} - \frac{M_a}{Z_{air}h}\right) \quad (27)$$

such that

$$Y_{aj} = \frac{D_{air}Z_{air}}{\delta_{bl}} \quad (28)$$

The transfer factors between the air and each surface compartment are listed in Table 3.

Transfers from Treated Region. When first treated, a surface will have pure compound in solution on the surface. The maximum concentration in the gas phase immediately adjacent to the surface is the vapor pressure of the compound. Thus, the maximum mass-transfer rate is

$$\text{mass-transfer rate} = SA_j \times \frac{D_{air}}{\delta_{bl}}\left(\frac{VP}{R_cT_m} - C_{air,a}\right) \quad (29)$$

where SA_j is the surface area of the treated region (m^2). We assume the concentration in the bulk gas phase is negligible relative to that at the interface. The mass-transfer rate is equal to the product of M_{it} and T_{it_ap} using the notation from eq 1.

In the current realization of the model, we do not track the mass in the treated compartments but rather use the mass-transfer rate as a source term to the air compartment and hence the fugacity model in the treated room for the first 4 d following the application. Over time, the compound will gradually diffuse into the material, and the gas-phase concentration over the treated region will no longer be the vapor pressure of the compound. The gas-phase concentration will be reduced and depend on the partition coefficient of the application surface and the rate of diffusion into the surface. Pesticides are often applied to both vinyl and wooden surfaces such as cabinets. At this point, we lack sufficient data to determine the flux rate from the treated surface and approximate it as one-half the rate resulting from eq 29 for times greater than 4 d post-application.

In the case of a compound with an extremely low vapor pressure, the transfer from the treated region may be dominated by resuspension of dust, the advective transport process from surfaces. The equivalent source rate to air can be estimated as the product of the advective transfer rate from the surface multiplied by the applied mass.

Degradation Rate Constants. Pesticides in air degrade by reaction with OH radicals. OH radical concentrations in indoor air are typically less than outdoor daytime levels. We base indoor OH radical concentrations on work by Sarwar et al. (*52*) using a modeling approach, and our distribution is listed in Table 1. These concentrations are multiplied by the chemical-specific second-order OH radical rate constant to yield the pseudo-first-order rate constant in air. If there is a known reaction or degradation rate constant for a surface, it can be included in the total loss-rate constant. However, at this time we do not have enough data to include surface degradation in the model.

Resulting Mass Distribution. The transfer factors are calculated in Excel. The compartment masses are determined

TABLE 5. Chemical Properties[a]

		chlorpyrifos	diazinon	permethrin
molecular weight (g/mol)	MW	351 (0)	304 (0)	391 (0)
octanol−water partition coefficient	K_{ow}	84000 (0.6)	3720 (1.1)	2.1×10^6 (0.7)
melting point (K)	T_m	315 (−)	liquid	307 (−)
vapor pressure (Pa)	VP	2.5×10^{-3} (0.9)	0.013(0.4)	1.8×10^{-5} (1.5)
solubility (mol/m^3)	S	2.4×10^{-3} (0.8)	0.17 (0.27)	0.19 (1.2)
Henry's law constant (Pa·m^3/mol)	H	0.37 (0.2)	0.025 (1.1)	0.01 (0.7)
diffusion coefficient in pure air (m^2/d)	D_{air}	0.46 (0.1)	0.46 (0.1)	0.46 (0.1)
OH radical reaction rate cnst (cm^3/mol d)	k_{OH}	3.3×10^{-6} (1.0)	8.4×10^{-6} (1.0)	−

[a] Coefficient of variation in parentheses.

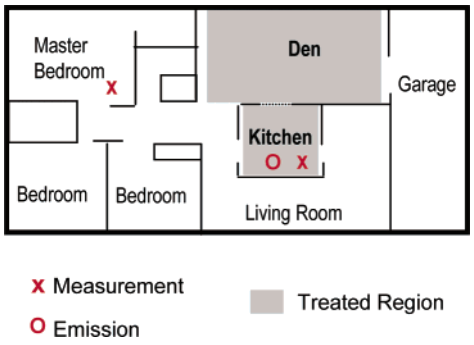

FIGURE 5. Layout of EPA test house.

using the Moderately Stiff/Trapezoidal solver in the MATLAB Simulink program.

Case Study

To demonstrate the model, we simulated a case study that was conducted in the U.S. EPA's Indoor Air Quality Test House in Cary, NC (*8*). The one-story test house received a chlorpyrifos crack-and-crevice application in the uncarpeted kitchen, as shown in Figure 5. We chose this case study for model comparison because it was conducted under known, documented conditions that we could simulate. Air concentrations and carpet loadings in various rooms were measured before and at 1, 3, 7, 14, and 21 d post-application. Model parameters approximate the test house configuration (as shown in Table 4). We compared modeled and measured concentrations in the air in both the treated region and bedroom and the carpet concentrations in the bedroom. (We were unable to compare carpet concentrations in treated regions due to high concentrations before the application resulting from a broadcast application 7 yr prior). For comparison, we ran the model for diazinon and permethrin to portray the differences that could be expected for those pesticides on the basis of their physical−chemical properties.

In each case, we assume an applied pesticide mass of 1.29 g, as applied in the test house. We estimate the area of application based on an approximate spray width of 5 cm and an approximate length of application of 15 m for a total area of 0.75 m^2, as indicated in Table 4.

Chemical Properties. There are significant differences in reporting pesticide properties (*54*). For most of the properties, we use the average and coefficient of variation for values listed in ref *54*, presented in Table 5 (values listed multiple times based on the same original source were only counted once, and values were checked to make sure units were properly converted from the original source; details can be found in the Supporting Information) (*54*). Since vapor pressure was thought to be highly influential, original sources were obtained for chlorpyrifos where possible and used to generate the mean and coefficient of variation (*55*−*59*). The reaction rate constants with OH radicals were determined based on the rate constants in ref *60*.

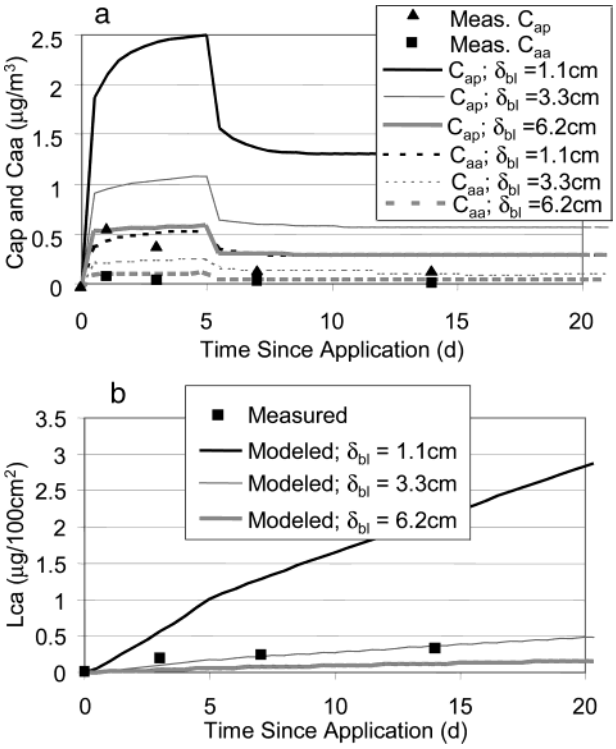

FIGURE 6. (a and b) Chlorpyrifos air concentrations and carpet loadings along with the measured values in each compartment.

We have chosen not to use a reaction rate constant for any of the surfaces for the pesticides. We reviewed literature on reaction rates in soil, and they were only significant for damp soils with significant levels of microorganisms (*61*). Because these conditions do not apply to indoor environments, we determined that it is appropriate to exclude degradation on surfaces in this paper.

Uncertainty Analysis. Three activities were completed in the uncertainty analysis. First, we completed a Monte Carlo simulation allowing all of the input parameters listed in Tables 1, 2, and 5 to vary. These Monte Carlo simulations are completed in two phases. Crystal Ball is used in Excel to sample from the input distributions and determine the resulting values of the transfer factors in Table 3. The resulting transfer factors are run through Simulink using a MATLAB interface to determine the resulting distributions of concentrations in each compartment of the model. We use 250 Latin hypercube simulations with 50 simulations in each bin. While this is unlikely to produce the full range of output, it is enough to begin to define the distribution.

Second, to assess the uncertainty associated with the release rate from the source, we completed three runs varying the release rate from the source assuming three boundary-layer thicknesses of 3.3, 1.1, and 6.2 cm, which are the mean value, the 10th and 90th percentile of the boundary-layer

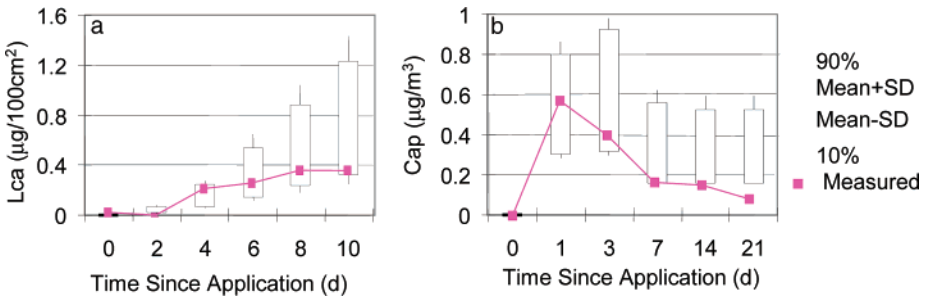

FIGURE 7. (a and b) Uncertainty results for an application of chlorpyrifos as compared to measured results.

thickness distribution, respectively. The point values for all of the parameters listed in Tables 1, 2, and 5 are used with the exception of the boundary-layer thickness, which uses the same value as used to calculate the release rate from the source region.

Third, a sensitivity analysis was completed with 1000 simulations to determine the rank correlation coefficients between the concentrations in air and carpet compartments for specified points in time and all the inputs in Tables 1, 2, and 5. The rank correlation coefficients measure the strength of the linear relationship between each input and the output, considering both the range of uncertainty of an input and the influence of that input on the concentration. We complete this for four time steps (1, 5, 25, and 50 d after application) to see if there are any changes in relative ranking.

Results and Discussion

Figure 6 shows results of the chlorpyrifos simulations along with data from the Stout and Mason study (*8*) for air measurements in both the primary (application) zone and the adjoining nontreated zone (bedroom) and carpet loading (L_{ca}, μg/100 cm^2) in the bedroom for the three boundary-layer conditions. There is a drop in the air concentration at the end of the 4th day due to our assumption that the source rate from the treated region is decreased on this day. If diffusion were modeled, it is expected that there would be a continuous decrease rather than a sharp drop.

The chlorpyrifos results of this comparison are encouraging because of the relatively close agreement between model output and measured carpet concentrations for a boundary layer of 3.3 cm. The modeled air concentrations are higher than the measured ones, matching more closely with a thicker boundary layer but not by more than a factor of 3. The thinner the boundary layer, the greater the concentration in both air (due to a greater relative source as the compound diffuses more readily from the treated region) and carpet (due to the increased transfer rate to carpet coupled with the increased air concentration). Figure 7 shows the modeled concentration distributions from the Monte Carlo simulations in the air in the treated region and the carpet in the untreated region. If one compares the range of concentration uncertainty bars with the difference between the concentrations from the different boundary layer thickness in Figure 6, they will see that the uncertainties associated with the parameter values and the boundary layer thickness and hence relative source strength, are comparable. Including the other uncertainties skews the distribution of the loading on carpet to higher values.

There are several reasons that the modeled concentrations may be higher than the measured concentrations. First, the boundary layer during the experiment might be greater than the mean value as the home was unoccupied, which would minimize human activity, thereby increasing the boundary layer. Second, the vapor pressure of the compound at the surface could be lower than the compound's vapor pressure as the active ingredient is mixed with various inert ingredients,

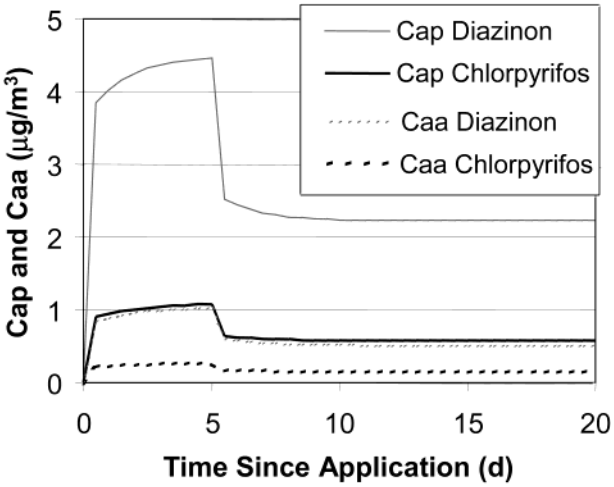

FIGURE 8. Comparison between chlorpyrifos and diazinon air concentrations following an application.

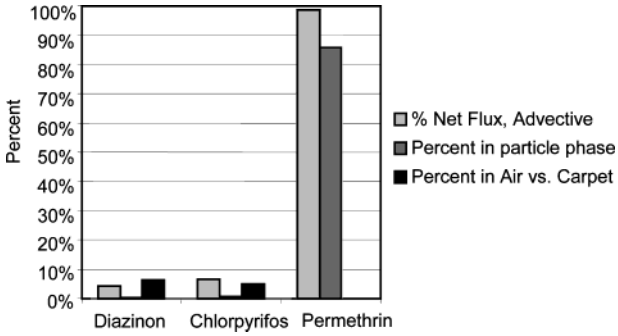

FIGURE 9. Percent of net flux through advective pathways, percent of the compound in air that is in the particle phase, and percent of the compound found in the air compartment.

effectively lowering the transfer rate from the treated region. The effect of the inert ingredients on the vapor pressure of the compound are unclear. Additionally, there could be significant diffusion into the treated surface, hence lowering the transfer rate from the surface.

The diazinon and chlorpyrifos air concentrations in both treated and untreated zones are shown in Figure 8. Note the higher concentrations for diazinon as it is more volatile than chlorpyrifos. Permethrin concentrations are not shown on the figure and remain fixed at 0.05 μg/m^3 in the treated region and 0.008 μg/m^3 in the nontreated region. They are significantly lower due to the low vapor pressure of this compound. They also remain fixed as opposed to dropping because the majority of the transport to the air is through the resuspension of particles. We compare the fraction of pesticides transported from surfaces to the air through advective particle-bound transport processes between the three compounds in Figure 9. We selected 5 d post-application for the comparison. We also compared the percent of airborne pesticide in the

TABLE 6. Results of Sensitivity Analysis for Both Mass in Air and Carpet in the Treated and Untreated Rooms

	M_{ap}		M_{aa}		M_{cp}		M_{ca}
	1 d	25 d	25 d		1 d	25 d	25 d
Chlorpyrifos							
AE	0.35	0.31	0.29	δ_{bl}	0.38	0.31	0.13
δ_{bl}	0.10	0.12	0.12	AE	0.15	0.24	0.19
k_{OH}	0.02	0.03	0.03	k_{OH}		0.01	0.01
Diazinon							
AE	0.33	0.32	0.30	δ_{bl}	0.40	0.36	0.24
δ_{bl}	0.09	0.09	0.10	AE	0.16	0.21	0.29
k_{OH}	0.12	0.13	0.13	k_{OH}	0.04	0.06	0.10
Permethrin							
$\rho_{p,65}$	0.20	0.19	0.18	AE	0.27	0.34	0.62
AE	0.14	0.15	0.13	$\rho_{p,65}$	0.17	0.16	
$v_{v,65}$	0.13	0.13	0.11	$\rho_{p,1}$	0.11	0.11	
$\rho_{p,10}$	0.11	0.10	0.10	K_{ow}	0.08	0.07	
$\rho_{p,1}$	0.06		0.05				

particulate phase and percent of total mass in the air. One can see the difference in the behavior of permethrin relative to the organophosphates, indicating the importance of the movement of dust in the home to characterize compounds with extremely low volatility.

The rank correlation coefficients based on both 1 and 25 d post-application concentrations for each compound are shown in Table 6. We first consider the concentration in air for which the main contributor to variance for the organophosphates is the air-exchange rate. This is followed by the boundary-layer thickness in the case of chlorpyrifos and the reaction rate constant in air for diazinon (in the sensitivity study, we combine the effects of OH radical reaction rate constant and OH radical concentration). Diazinon is more reactive in air, increasing the importance of this removal rate constant. The parameter with the largest contribution to variance for the mass in carpet in the adjoining room is the boundary-layer thickness of air over carpet, followed by the air-exchange rate. The air-exchange rate is truly variable between homes, while the boundary-layer thickness is both variable and uncertain. There are some slight variations in the contribution to variance numbers between the 1 d post-application and later time steps, as shown for the carpet and air in the primary application region.

The results of the sensitivity analysis are quite different for permethrin, with many of the properties of dust explaining a significant portion of the variance. The air-exchange rate is still important, but additionally the mass of particles in air and the deposition rate are important for this compound. These values are uncertain, and more research should be completed to better quantify these parameters. This corresponds with the results shown in Figure 9, indicating the relative importance of dust as a transfer pathway.

A better understanding of pesticide fate and transport in indoor environments is needed to quantify exposure to pesticides used indoors. A general framework for modeling fate and transport indoors is presented. A main challenge is to better understand mass transfer from treated surfaces. The case study results are on the same order of magnitude as measured results, although it appears as though we have overestimated the source emission rate from the treated region. Properly accounting for diffusion into the surface and considering the concentration profile in the surface may improve the results. More data are clearly needed to understand transport from the treated regions. To use this model for assessing exposures, the transferable surface residues relative to total mass need to be determined. Then, the model can be used in conjunction with exposure models that consider human contact with air and surfaces.

Acknowledgments

The United States Environmental Protection Agency through its Office of Research and Development partially funded and collaborated in the research described here under assistance agreement number DW-988-38190-01-0 to Lawrence Berkeley National Laboratory through the U.S. Department of Energy under Contract Grant DE-AC03-76SF00098 and partially conducted at Harvard School of Public Health. It has been subjected to Agency review and approved for publication. D.H.B. also acknowledges general support of her research under the NIEHS Center for Environmental Health ES000002. The authors also thank T. E. McKone, D. Stout, R. L. Corsi, W. W. Nazaroff, C. Seigel, and our thoughtful reviewers for their helpful inputs, programming assistance, and constructive comments.

Supporting Information Available

Additional information on the derivation of the partition coefficients for vinyl and carpet, the diffusive transfer rate to surfaces, and the derivation of the mean values and coefficient of variations for the parameters in Tables 1, 2, and 5. This material is available free of charge via the Internet at http://pubs.acs.org.

Literature Cited

(1) Gordon, S.; Callahan, P.; Nishioka, M.; Brinkman, M.; O'Rourke, M.; Lebowitz, M.; Moschandreas, D. *J. Exposure Anal. Environ. Epidemiol.* **1999**, *9*, 456−470.
(2) Zartarian, V. G.; Ozkaynak, H.; Burke, J. M.; Zufall, M. J.; Rigas, M. L.; Furtaw, E. J. *Environ. Health Perspect.* **2000**, *108*, 505−514.
(3) Gurunathan, S.; Robson, M.; Freeman, N.; Buckley, B.; Roy, A.; Meyer, R.; Bukowski, J.; Lioy, P. *Environ. Health Perspect.* **1998**, *106*, 9−16.
(4) Akland, G.; Pellizzari, E.; Hu, Y.; Roberds, M.; Rohrer, C.; Leckie, J.; Berry, M. *J. Exposure Anal. Environ. Epidemiol.* **2000**, *10*, 710−722.
(5) Leidy, R.; Wright, C.; Dupree, H. J. In *Pesticides in Urban Environments*; Racke, K., Leslie, A., Eds.; American Chemical Society: Washington, DC, 1993.
(6) Byrne, S. L.; Shurdut, B. A.; Saunders, D. G. *Environ. Health Perspect.* **1998**, *106*, 725−731.
(7) Lewis, R. G.; Fortune, C. R.; Blanchard, F. T.; Camann, D. E. *J. Air Waste Manage. Assoc.* **2001**, *51*, 339−351.
(8) Stout, D. M.; Mason, M. In *Indoor Air 2002*: Monterey, CA, 2002; Vol. 4, pp 984−899.
(9) Berger-Preis, E.; Preis, A.; Seilaff, K.; Meththild, R.; Ilgen, B.; Levsen, K. *Indoor Air* **1997**, *7*, 248−261.
(10) Mackay, D.; Paterson, S. *Chemosphere* **1983**, *12*, 143−154.
(11) Matoba, Y.; Yoshimur, J.; Ohnishi, J.; Mikami, N.; Matsuo, M. *J. Air Waste Manage. Assoc.* **1998**, *48*, 969−978.
(12) Neretnieks, I.; Christiansson, J.; Romero, L.; Dagerholt, L.; Yu, J. *Indoor Air* **1993**, *3*, 2−11.
(13) Won, D.; Corsi, R. L.; Rynes, M. *Indoor Air* **2001**, *11*, 246−256.
(14) Won, D. Y.; Corsi, R. L.; Rynes, M. *Environ. Sci. Technol.* **2000**, *34*, 4193−4198.
(15) Cox, S. S.; Little, J. C.; Hodgson, A. T. *J. Air Waste Manage. Assoc.* **2001**, *51*, 1195−1201.
(16) Cox, S. S.; Zhao, D. Y.; Little, J. C. *Atmos. Environ.* **2001**, *35*, 3823−3830.
(17) Jorgensen, R. B.; Bjorseth, O. *Environ. Int.* **1999**, *25*, 17−27.
(18) Jorgensen, R. B.; Bjorseth, O.; Malvik, B. *Indoor Air* **1999**, *9*, 2−9.
(19) Jorgensen, R. B.; Dokka, T. H.; Bjorseth, O. *Indoor Air* **2000**, *10*, 27−38.
(20) Little, J. C.; Hodgson, A. T.; Gadgil, A. J. *Atmos. Environ.* **1994**, *28*, 227−234.
(21) Meininghaus, R.; Gunnarsen, L.; Knudsen, H. N. *Environ. Sci. Technol.* **2000**, *34*, 3101−3108.
(22) Van Loy, M. D.; Riley, W. J.; Daisey, J. M.; Nazaroff, W. W. *Environ. Sci. Technol.* **2001**, *35*, 560−567.
(23) VanLoy, M. D.; Lee, V. C.; Gundel, L. A.; Daisey, J. M.; Sextro, R. G.; Nazaroff, W. W. *Environ. Sci. Technol.* **1997**, *31*, 2554−2561.
(24) VanderWal, J. F.; Hoogeveen, A. W.; Wouda, P. *Indoor Air* **1997**, *7*, 215−221.
(25) vanderWal, J. F.; Hoogeveen, A. W.; vanLeeuwen, L. *Indoor Air* **1998**, *8*, 103−112.

(26) Mackay, D. *Multimedia Environmental Models, the Fugacity Approach*; Lewis Publishers: Chelsea, MI, 2001.
(27) Lewis, R. G.; Fortune, C. R.; Willis, R. D.; Camann, D. E.; Antley, J. T. *Environ. Health Perspect.* **1999**, *107*, 721−726.
(28) Kissel, J. C. *Risk Anal.* **1995**, *15*, 613−614.
(29) Rodes, C. E.; Newsome, J. R.; Vanderpool, R. W.; Antley, J. T.; Lewis, R. G. *J. Exposure Anal. Environ. Epidemiol.* **2001**, *11*, 123−139.
(30) Finizio, A.; Mackay, D.; Bidleman, T.; Harner, T. *Atmos. Environ.* **1997**, *31*, 2289−2296.
(31) Harner, T.; Bidleman, T. F. *Environ. Sci. Technol.* **1998**, *32*, 1494−1502.
(32) Bennett, D. H.; Scheringer, M.; McKone, T. E.; Hüngerbuhler, K. *Environ. Sci. Technol.* **2001**, *35*, 1181−1189.
(33) Offenberg, J. H.; Baker, J. E. *Atmos. Environ.* **2000**, *34*, 1509−1517.
(34) Vohrees, D. J. *Environmental Health*; Harvard School of Public Health: Boston, MA, 1996; p 200.
(35) Ferguson, J. E.; Kim, N. D. *Sci. Total Environ.* **1991**, *100*, 125−150.
(36) Riley, W. J.; McKone, T. E.; Lai, A. C. K.; Nazaroff, W. W. *Environ. Sci. Technol.* **2002**, *36*, 200−207.
(37) Long, C. M.; Suh, H. H.; Koutrakis, P. *J. Air Waste Manage. Assoc.* **2000**, *50*, 1236−1250.
(38) Tichenor, B.; Guo, Z.; Dunn, J.; Sparks, L.; Mason, M. *Indoor Air* **1991**, *1*, 23−35.
(39) Won, D. Civil and Environmental Engineering, University of Austin: Austin, TX, 2000.
(40) Diamond, M. L.; Gingrich, S. E.; Fertuck, K.; McCarry, B. E.; Stern, G. A.; Billeck, B.; Grift, B.; Brooker, D.; Yager, T. D. *Environ. Sci. Technol.* **2000**, *34*, 2900−2908.
(41) Thatcher, T. L.; Layton, D. W. *Atmos. Environ.* **1995**, *29*, 1487−1497.
(42) Leese, K. E.; Hall, R. M.; Cole, E. C.; Foarde, K. K.; Berry, M. A. *U.S. EPA and Waste Management Association's International Symposium*: *Measurement of Toxic and Related Air Pollutants*, Durham, NC, 1993; pp 82−87.
(43) Fortune, C. R.; Blanchard, F. T.; Ellenson, W. D. *Analysis of aged in-home carpeting to determine the distribution of pesticide residues between dust, carpet, and pad compartments*; EPA-NERL: 2000.
(44) Edwards, R. D.; Yurkow, E. J.; Lioy, P. J. *Sci. Total Environ.* **1998**, *224*, 69−80.
(45) Murray, D. M.; Burmaster, D. E. *Risk Anal.* **1995**, *15*, 459−465.
(46) Miller, S. L.; Leiserson, K.; Nazaroff, W. W. *Indoor Air* **1997**, *7*, 64−75.
(47) Rodes, C. E.; Peters, T. M.; Lawless, P. A.; Wallace, L. In *Abstracts of the 6th Annual Meeting of the International Society of Exposure Analysis*, New Orleans, 1996.
(48) Ferro, A. R.; Kopperud, R. J.; Hildemann, L. M. *Indoor Air 2002*; Monterey, CA, 2002; Vol. 2, pp 527−532.
(49) Nazaroff, W. W.; Alvarez-Cohen, L. *Environmental Engineering Science*; John Wiley & Sons: New York, 2001.
(50) Lai, A. C. K.; Nazaroff, W. W. *J. Aerosol Sci.* **2000**, *31*, 463−476.
(51) Morrison, G. C. Department of Engineering, University of California, Berkeley, CA, 1999, 303 pp.
(52) Sarwar, G.; Corsi, R. L.; Kimura, Y.; Allen, D.; Weschler, C. J. *Atmos. Environ.* **2002**, *36*, 3973−3988.
(53) Woodrow, J. E.; Seiber, J. N.; Dary, C. *J. Agric. Food Chem.* **2001**, *49*, 3841−3846.
(54) Mackay, D.; Shiu, W. Y.; Ma, K. C. *Illustrated Handbook of Physical−Chemical Properties and Environmental Fate for Organic Chemicals*; Lewis Publishers: Boca Raton, 1997; Vol. 5, Pesticide Chemicals.
(55) Hinckley, D. A.; Bidleman, T. F.; Foreman, W. T. *J. Chem. Eng. Data* **1990**, *35*, 232−237.
(56) Kim, Y. H.; Woodrow, J. E.; Seiber, J. N. *J. Chromatogr* **1984**, *314*, 37−53.
(57) Hamaker, J. W. In *Environmental Dynamics of Pesticides*; Haque, R., Freed, V. H., Eds.; Plenum Press: New York, 1975; pp 115−133.
(58) Brust, H. F. *Down Earth* **1966**, *22*, 21−22.
(59) Eichler, W., Ed. *Handbuch der Insektizidkunde*; Veb Verlag Volk und Gesundheit: Berlin, 1965. As cited in ref *54*.
(60) Howard, P. H.; Ed. *Handbook of Environmental Fate and Exposure Data for Organic Chemicals, Pesticides, Vol. III*; Lewis Publishers: Chelsea, MI, 1991.
(61) Montgomery, J. H. *Agrochemicals Desk Reference. Environment Data*; Lewis Publishers: Chelsea, MI, 1993.

Received for review March 31, 2003. Revised manuscript received December 22, 2003. Accepted January 6, 2004.

ES034287M